Dumas, D.C.S., Gallacher, K., Millar, R., MacLaren, I., Myronov, M., Leadley, D.R., and Paul, D.J (2014) *Silver antimony Ohmic contacts to moderately doped n-type germanium.* Applied Physics Letters, 104 (16). p. 162101. ISSN 0003-6951

Copyright © AIP Publishing LLC

http://eprints.gla.ac.uk/93348/

Deposited on: 02 May 2014

Enlighten – Research publications by members of the University of Glasgow
http://eprints.gla.ac.uk

# Silver antimony Ohmic contacts to moderately-doped n-type germanium

D.C.S. Dumas,[1] K. Gallacher,[1] R.Millar,[1] I. MacLaren,[2] M. Myronov,[3] D.R. Leadley,[3] and D.J. Paul[1, a)]

[1)] *University of Glasgow, School of Engineering, Rankine Building, Oakfield Avenue, Glasgow, G12 8LT, U.K.*

[2)] *University of Glasgow, SUPA School of Physics and Astronomy, Kelvin Building, University Avenue, Glasgow, G12 8QQ, U.K.*

[3)] *University of Warwick, Department of Physics, Coventry, CV4 7AL, U.K.*

A self doping contact consisting of a silver/antimony alloy that produces an Ohmic contact to moderately doped n-type germanium (doped to a factor of four above the metal-insulator transition) has been investigated. An evaporation of a mixed alloy of Ag/Sb (99%/1%) onto n-Ge ($N_D = 1 \times 10^{18}$ cm$^{-3}$) annealed at 400°C produces an Ohmic contact with a measured specific contact resistivity of $(1.1 \pm 0.2) \times 10^{-5}$ Ω-cm$^2$. It is proposed that the Ohmic behaviour arises from an increased doping concentration at the Ge surface due to the preferential evaporation of Sb confirmed by transmission electron microscope analysis. It is suggested that the doping concentration has increased to a level where field emission will be the dominate conduction mechanism. This was deduced from the low temperature electrical characterisation of the contact, which exhibits Ohmic behaviour down to a temperature of 6.5 K.

PACS numbers: 73.40.Cg, 73.40.Gk, 73.63.Rt
Keywords: metal-semiconductor contacts, germanium

There is an increasing interest in using Ge for both electronic and optical devices on Si substrates to expand the functionality of Si technology. Ge is an attractive material for use in many different technologies including end-of-roadmap complementary metal-oxide semiconductor (CMOS), where its higher carrier mobilities compared to Si would potentially allow for reduced power operation.[1] Ge integration has benefits for Si photonics devices[2] such as photodetectors[3], single photon avalanche detectors[4], modulators[5] and Ge lasers[6]. Ge has also been used for spintronic devices[7] along with thermoelectrics[8] and there have been proposals for Ge/SiGe quantum cascade lasers.[9]

Poor electrical contacts to n-Ge are a potential roadblock to the majority of these applications. Low resistive Ohmic contacts to n-Ge are difficult to achieve because of strong Fermi level pinning at the charge neutral level (0.08 to 0.09 eV),[10,11] just above the valence band (Fig.1). This produces a large Schottky barrier height at the metal-Ge interface[12], which is relatively independent of the metal work function (pinning factor S=0.02 to 0.05).[10,11] Whilst the cause of the Fermi level pinning is not fully understood, multiple methods to overcome the pinning and form an Ohmic contact have been suggested. Degenerately in-situ P doped n-Ge can support Ohmic contacts to annealed Ni[13,14]. The large dopant concentration, however, required to achieve Ohmic behaviour results in segregation of the n-type dopants during chemical vapor deposition (CVD) which is detrimental for many vertical devices since any other epitaxial layers subsequently grown will be unintentionally doped.[15] Other methods investigated include lowering the barrier height by ion implantation[16,17], inserting an interfacial layer,[12,18–20] and the deposition of Yb capped with $SiO_2$[21]. AgSb alloys have been shown to form Ohmic contacts to low Ge concentration n-type $Si_{1-x}Ge_x$ alloys,[22] leading to the investigation of AgSb for this moderately doped n-Ge layer. The method described in this paper allows a simple fabrication process to form an Ohmic contact to n-Ge doped just above the metal-insulator transition compared to alternative methods.

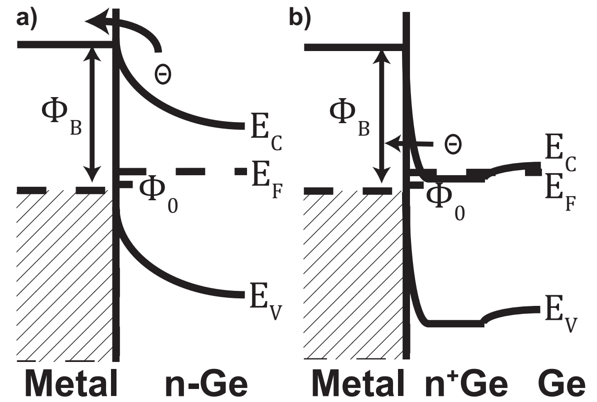


FIG. 1. A schematic diagram of a metal contact to low or moderately doped n-Ge, where the Fermi level is pinned near the charge neutral level just above the valence band. Therefore, a large Schottky barrier results, regardless of the metal work function. (b) The ideal case where the Ge is sufficiently doped to reduce the barrier width to allow tunnelling of electrons through the barrier to form an Ohmic contact.

The n-Ge was epitaxially grown using an ASM Epsilon 2000E low pressure CVD tool on a p$^-$ Si(001) wafer.[23] The Ge layer was 2 μm thick and a phosphane precursor produced an in-situ P doping of $1 \times 10^{18}$ cm$^{-3}$. The electrically activated dopant concentration was subsequently confirmed by Hall effect measurements on mesa etched Hall bar samples. The Mott criteria for Ge:P is $2.5 \times 10^{17}$

[a)] Electronic mail: Douglas.Paul@glasgow.ac.uk

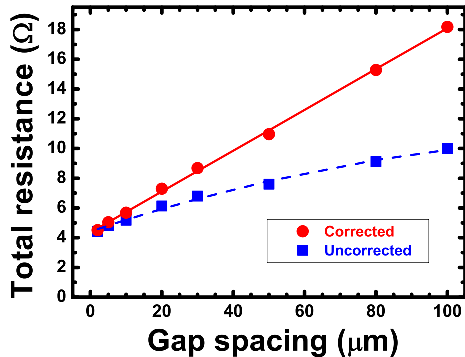


FIG. 2. The measured and corrected resistance values for a Ag/Sb (99%/1%) alloy on n-Ge CTLM structure with 50 $\mu$m radius annealed at 400°C with a linear fit applied to the corrected values.

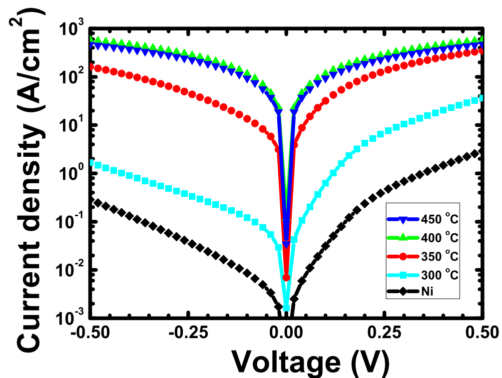


FIG. 3. The semi-log current density versus voltage characteristics for a 90 nm 99% Ag / 1% Sb alloy on n-Ge annealed at 300-550°C. The NiGe sample annealed at 340°C is also shown (black line). The AgSb on n-Ge contacts annealed at 400 and 450°C for 5 min are clearly Ohmic.

cm$^{-3}$ (Ref. 24) indicating that the sample is metallic with a doping level that is a factor of 4 above the metal-insulator transition.

15 mm$^2$ chips for electrical measurements were prepared by first cleaning in acetone, followed by a rinse in propan-2-ol, and then blown dry in $N_2$. Circular transfer length method (CTLM) structures[25] were then patterned in poly(methyl methacrylate) using a Vistec VB6 electron beam lithography tool to produce devices with a placement accuracy of  1 nm. The samples were then dipped in a 5:1 buffered HF solution to remove any native oxide, before being immediately placed into a metal evaporator and pumped down to $< 1 \times 10^{-6}$ mbar, where 90 nm of a mixed Ag/Sb (99%/1%) alloy was deposited by thermal evaporation. Following lift-off, the samples were annealed for 5 minutes in $N_2$ in a rapid thermal annealer at temperatures from 300-550°C. For comparison, a reference sample was produced with 100 nm of electron-beam evaporated Ni and annealed at 340°C for 30 s. Since Ni on Ge produces a germanide phase (NiGe) that has the lowest resistivity out of all the transition metals[26], it is often used to make a contact to n-Ge and to date has resulted in the lowest values of specific contact resistivity ($\rho_c$) when formed at 340 °C.[14] This approach, however, requires highly doped Ge ($N_D > 1 \times 10^{19}$ cm$^{-3}$), where conduction is dominated by field emission through a thin Schottky barrier. Therefore, for lower doped n-Ge such as the material investigated in this work, it is anticipated that a Schottky contact will form because conduction will be reliant on thermionic emission over the barrier (Fig. 1).

Each chip contained multiple CTLM structures with inner radii ranging from 50 to 100 $\mu$m and gap spacings ranging from 2 $\mu$m to 100 $\mu$m. The CTLM structures were characterised using a four connection (separate force and sense for voltage and current) dc configuration with a voltage sweep from -2 to 2 V using an Agilent B1500 semiconductor parameter analyser. Unlike linear TLM structures the CTLMs can be fabricated in a single lithography step since they do not require a mesa etch to confine the current path. Therefore, this removes errors related to lithographic misalignment between the mesa etch and contact deposition. The total resistance of each structure is measured and then plotted as a function of the gap spacing. Surface passivation was not deposited onto these devices as previous work with Ge single photon avalanche detectors has indicated no change to the dark current on the deposition of $SiO_2$ or $Si_3N_4$ surface passivation.[4] A geometric correction factor[25] is required such that the resistance divided by the correction factor is a linear function of the gap spacing, which allows a linear fit to the data (Fig. 2). From this the sheet resistance ($R_{sh}$) and the transfer length ($L_T$) can be extracted. The $\rho_c$ is then calculated by using[25]

$$\rho_c = L_T^2 \times R_{sh} \tag{1}$$

Figure 3 shows the current-voltage (IV) characteristics of 50 $\mu$m radius CTLM structures with 100 $\mu$m gap spacing for the AgSb contacts annealed at 300-550°C for 5 min. For comparison the NiGe contact is also plotted. It is obvious that the AgSb contacts annealed at 300°C and 350°C both demonstrate Schottky behaviour. Both show better current conduction, however, compared to the NiGe contact, implying that some of the Sb has been activated by the anneal. The contacts annealed at 400°C and 450°C are clearly Ohmic, (Fig. 3) as characterised by the symmetry and high current density for the forward and reverse biases. This suggests that more Sb has become electrically active and the n-Ge dopant concentration has increased to a level where field emission dominates conduction. Anneal temperatures higher than 450°C resulted in agglomeration of the contact, which is evident in the atomic force microscopy image in Fig. 4.

Since the AgSb contacts annealed at 400°C and 450°C

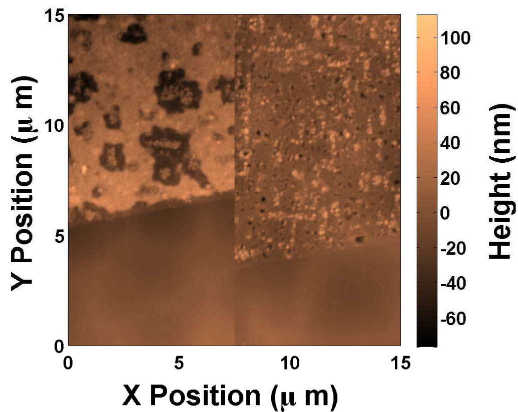


FIG. 4. Surface roughness map of the AgSb on n-Ge contact annealed at 500°C (left) and 550°C (right) measured with an atomic force microscope. The smooth surface in the bottom of the figure corresponds to an area of blank Ge without the AgSb alloy.

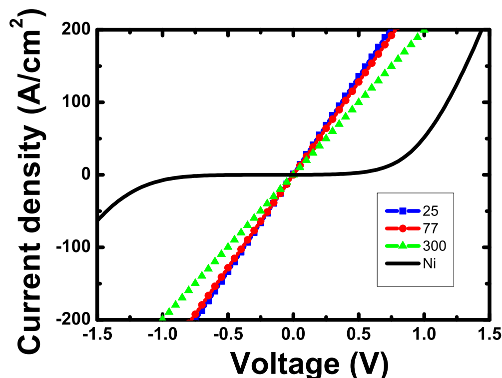


FIG. 5. The current versus voltage characteristics measured at different temperatures for a 90 nm AgSb alloy on n-Ge contact annealed at 400°C for 5 min. For comparison the room temperature IV for the NiGe contact annealed at 340°C is displayed (black line).

were Ohmic, the $\rho_c$ was extracted from the CTLM structures and are summarised in table I. The best result was obtained for a AgSb alloy on n-Ge contact annealed at 400°C for 5 min. The contact was shown to be stable up to an anneal time of 10 minutes. The IV characteristics of the contact was measured as a function of sample temperature and this is shown in Fig. 5. It is clear that the contact remains Ohmic down to the base temperature of the measurement cryostat of 6.5 K. There is noticeable improvement in the current conduction for the IVs at 6.5 K and 77 K compared to room temperature, which can be explained from an increase in conductivity for the as grown n-Ge at lower temperatures.[27] The Ohmic behaviour at 77 K and below is another indication that field emission is the dominant conduction mechanism. Therefore, this implies that the doping concentration of the

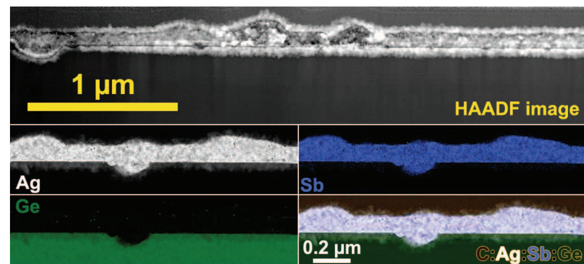


FIG. 6. HAADF images of a AgSb on n-Ge contact annealed at 400°C for 5 minutes.

n-Ge under the contact has been increased due to the Sb evaporation and subsequently electrically activated from the anneal. Since the solid solubility limit of Sb in Ge is 5 orders of magnitude higher than Ag at these anneal temperatures[28] enhanced Sb doping at the metal / Ge interface is expected. To highlight this further the IV characteristics for the NiGe contact at room temperature are plotted in Fig.5 and is clearly rectifying.

Since the NiGe contact is rectifying, the Fermi level pinning can be obtained by calculating the Schottky barrier height ($\phi_B$)[29]

$$\phi_B = \frac{k_B T}{q} \ln\left(\frac{AA^* T^2}{I_S}\right) \tag{2}$$

where $k_B$ is the Boltzmann constant, $T$ is the temperature in K, $A$ is the area of the contact, $A^*$ is 143 $\mathrm{Acm^{-2}K^{-2}}$ for Ge[11], and $I_S$ is the current at zero bias extrapolated from the semi-log current versus voltage curve for the contact. From the IV characteristics of the NiGe contact (Figs. 3 and 5) a barrier height of $506 \pm 11$ meV was extracted, which is consistent with values previously measured.[10,11,30] Due to the large barrier height and low doping concentration ($1 \times 10^{18}$ $\mathrm{cm^{-3}}$) the NiGe contact is reliant on thermionic emission over the barrier (Fig. 1). This shows the advantage of this AgSb process, which is self-doping, in creating an Ohmic contact to moderately doped n-Ge by increasing the dopant concentration.

To investigate the AgSb contact annealed at 400°C in more detail, the contact was analysed using scanning transmission electron microscopy (STEM). Samples were prepared by the focused ion beam (FIB) lift-out process using a FEI Nova Nanolab 200 Dualbeam FIB microscope. STEM characterisation was then performed on the resulting sections using a JEOL ARM200F microscope equipped with a cold field emission gun electron source and a Gatan GIF Quantum electron energy loss spectrometer. Characterisation was performed using electrons accelerated to 200 kV, with images recorded using the high-angle annular dark-field (HAADF) mode and dual electron energy loss spectrum (DualEELS) images recorded over an energy range up to 2100 eV covering the edges for Ag $M_{4,5}$, Sb $M_{4,5}$ and Ge $L_{2,3}$, as well as C K. Quantification was performed using a new convolution-based approach provided by Gatan Inc.

| Anneal (°C) | Contact | $\rho_c$ ($\Omega$-cm$^2$) |
|---|---|---|
| 300 | Schottky | - |
| 350 | Schottky | - |
| 400 | Ohmic | $(1.1 \pm 0.2) \times 10^{-5}$ |
| 450 | Ohmic | $(1.7 \pm 0.3) \times 10^{-5}$ |
| 500 | Agglomerated | - |
| 550 | Agglomerated | - |

TABLE I. The contact type that arises for a AgSb alloy on n-Ge annealed at different temperatures. The specific contact resistivity is included for the Ohmic contacts.

(Pleasanton, USA) based on earlier work by Verbeeck et al.[31,32] which fits the fine structure at the absorption edges based on the low loss spectrum and thus accounts for multiple scattering explicitly through the use of the whole DualEELS dataset. The HAADF image of Fig. 6 shows a cross-section of a contact annealed at 400°C for 5 minutes. The distribution of the Ag, Sb and Ge are shown both separately and as a multicoloured overlay map. In both the image and the maps, it is clear that, unlike $Ni_xGe_y$ contacts[13], the AgSb forms a predominately flat contact on the surface, with just the occasional dip into the Ge. It is also observed that the Sb has diffused by $< 5$ nm into the Ge layer remaining predominantly on the surface of the semiconductor. The top surface of the contact is rougher. This is most likely due to the fact that the contact is polycrystalline with nanosized grains. One surprise is the composition of the contact, which is significantly different to the 99% Ag / 1% Sb composition of the target. The estimates from our DualEELS quantification suggest an approximate 75% Ag / 25% Sb composition suggesting that Sb is preferentially evaporated from the target, enriching it significantly in the film. This may also suggest that the composition would be graded in a thicker Ag contact through depletion of the Sb in the target.

To conclude, to reduce n-type dopant segregation during epitaxial growth, n-Ge Ohmic contact layers grown below nominally undoped active layers require lower doping concentrations than that required to produce low $\rho_c$ Ohmic contacts. The NiGe Ohmic contacts to n-Ge requires a highly doped layer ($N_D > 1 \times 10^{19}$ cm$^{-3}$), otherwise a Schottky contact forms. Other processes that have been demonstrated require additional steps, adding to the complexity of the contact scheme. A process for the creation of Ohmic contacts to n-Ge ($N_D = 1 \times 10^{18}$ cm$^{-3}$, which requires only a AgSb alloy deposition and an anneal has been demonstrated. A deposition of a AgSb alloy followed by a 400°C anneal for 5 minutes can produce an Ohmic contact with a $\rho_c$ of $(1.1 \pm 0.2) \times 10^{-5}$ $\Omega$-cm$^2$ on n-Ge layers doped to a factor of four above the metal insulator transition. The contacts remained Ohmic down to 6.5 K indicating that field emission is the main electrical conduction mechanism.

The authors would like to thank the staff of the James Watt Nanofabrication Centre for help with fabrication, the assistance of Mr W. Smith and Dr S. McFadzean in the Kelvin Nanocharacterisation Centre, and Dr P. Thomas of Gatan Inc. for assistance with the DualEELS quantification. The work was funded by UK EPSRC.

[1] R. Pillarisetty, Nature **479**, 324 (2011).
[2] D. J. Paul, Elec. Lett. **45**, 582 (2009).
[3] S. J. Koester, J. D. Schaub, G. Dehlinger, and J. O. Chu, IEEE J. Sel. Topics Quant. Elec. **12**, 1489 (2006).
[4] R. E. Warburton, G. Intermite, M. Myronov, P. Allred, D. R. Leadley, K. Gallacher, D. J. Paul, N. J. Pilgrim, L. J. M. Lever, Z. Ikonic, R. W. Kelsall, E. Huante-Ceron, A. P. Knights, and G. S. Buller, IEEE Trans. Elec. Dev. **60**, 3807 (2013).
[5] Y. H. Kuo, Y. K. Lee, Y. S. Ge, S. Ren, J. E. Roth, T. I. Kamins, D. A. B. Miller, and J. S. Harris, Nature **437**, 1334 (2005).
[6] R. E. Camacho-Aguilera, Y. Cai, N. Patel, J. T. Bessette, M. Romagnoli, L. C. Kimerling, and J. Michel, Opt. Exp. **20**, 11316 (2012).
[7] C. Shen, T. Trypiniotis, K. Y. Lee, S. N. Holmes, R. Mansell, M. Husain, V. Shah, X. V. Li, H. Kurebayashi, I. Farrer, C. H. de Groot, D. R. Leadley, G. Bell, E. H. C. Parker, T. E. Whall, D. A. Ritchie, and C. H. W. Barnes, Appl. Phys. Letts. **97**, 162104 (2010).
[8] L. F. Llin, A. Samarelli, S. Cecchi, T. Etzelstorfer, E. M. Gubler, D. Chrastina, G. Isella, J. Stangl, J. M. R. Weaver, P. S. Dobson, and D. J. Paul, Appl. Phys. Letts. **103**, 143507 (2013).
[9] D. J. Paul, Laser & Photonics Rev. **4**, 610 (2010).
[10] A. Dimoulas, P. Tsipas, A. Sotiropoulos, and E. K. Evangelou, Appl. Phys. Letts. **89**, 252110 (2006).
[11] T. Nishimura, K. Kita, and A. Toriumi, Appl. Phys. Letts. **91**, 123123 (2007).
[12] Y. Zhou, M. Ogawa, X. Han, and K. L. Wang, Appl. Phys. Letts. **93**, 202105 (2008).
[13] K. Gallacher, P. Velha, D. J. Paul, I. MacLaren, M. Myronov, and D. R. Leadley, Appl. Phys. Letts. **100**, 022113 (2012).
[14] K. F. Gallacher, P. Velha, D. J. Paul, I. Maclaren, M. Myronov, and D. R. Leadly, ECS Trans. **50**, 1081 (2013).
[15] J. Hartmann, V. Loup, G. Rolland, P. Holliger, F. Laugier, C. Vannuffel, and M. Semeria, J. Crystal Growth **236**, 10 (2002).
[16] M. Koike, Y. Kamata, T. Ino, D. Hagishima, K. Tatsumura, M. Koyama, and A. Nishiyama, J. Appl. Phys. **104**, 023523 (2008).
[17] G. Thareja, S. L. Cheng, T. Kamins, K. Saraswat, and Y. Nishi, IEEE Elec. Dev. Letts. **32**, 608 (2011).
[18] Z. Li, X. An, M. Li, Q. Yun, M. Lin, M. Li, X. Zhang, and R. Huang, IEEE Elec. Dev. Letts. **33**, 1687 (2012).
[19] J.-Y. J. Lin, A. M. Roy, A. Nainani, Y. Sun, and K. C. Saraswat, Appl. Phys. Letts. **98**, 092113 (2011).
[20] P. Paramahans Manik, R. Kesh Mishra, V. Pavan Kishore, P. Ray, A. Nainani, Y.-C. Huang, M. C. Abraham, U. Ganguly, and S. Lodha, Appl. Phys. Letts. **101**, (2012).
[21] Z.-W. Zheng, T.-C. Ku, M. Liu, and A. Chin, Appl. Phys. Letts. **101**, 223501 (2012).
[22] S. F. Nelson and T. N. Jackson, Appl. Phys. Letts. **69**, 3563 (1996).
[23] V. A. Shah, A. Dobbie, M. Myronov, and D. R. Leadley, Solid-State Elec. **62**, 189 (2011).
[24] P. P. Edwards and M. J. Sienko, Phys. Rev. B **17**, 2575 (1978).
[25] J. Klootwijk and C. Timmering, in *Proc. Int. Conf. Microelect. Test Struc.* (2004) pp. 247 – 252.
[26] S. Gaudet, C. Detavernier, A. Kellock, P. Desjardins, and C. Lavoie, J. Vac. Sci. Technol. A **24**, 474 (2006).
[27] C. S. Hung and J. R. Gliessman, Phys. Rev. **96**, 1226 (1954).
[28] F. Trumbore, Bell Systems Tech. J. **39**, 205 (1960).
[29] D. Schroder, *Semiconductor Material and Device Characterization* (IEEE Press, 2006).
[30] H. Yao, C. Tan, S. Liew, C. Chua, C. Chua, R. Li, R. Lee, S. Lee,

and D. Chi, in *Int. Workshop Junction Technol.* (2006) pp. 164–169.

[31] J. Verbeeck and S. Van Aert, Ultramicroscopy **101**, 207 (2004).

[32] J. Verbeeck, S. Van Aert, and G. Bertoni, Ultramicroscopy **106**, 976 (2006).